AJNR

Differential Gene Expression in Glioblastoma Defined by ADC Histogram Analysis: Relationship to Extracellular Matrix Molecules and Survival

W.B. Pope, L. Mirsadraei, A. Lai, A. Eskin, J. Qiao, H.J. Kim, B. Ellingson, P.L. Nghiemphu, S. Kharbanda, R.H. Soriano, S.F. Nelson, W. Yong, H.S. Phillips and T.F. Cloughesy

Differential Gene Expression in Glioblastoma Defined by ADC Histogram Analysis: Relationship to Extracellular Matrix Molecules and Survival

W.B. Pope
L. Mirsadraei
A. Lai
A. Eskin
J. Qiao
H.J. Kim
B. Ellingson
P.L. Nghiemphu
S. Kharbanda
R.H. Soriano
S.F. Nelson
W. Yong
H.S. Phillips
T.F. Cloughesy

BACKGROUND AND PURPOSE: ADC histogram analysis can stratify outcomes in patients with GBM treated with bevacizumab. Therefore, we compared gene expression between high-versus-low ADC tumors to identify gene expression modules that could underlie this difference and impact patient prognosis.

MATERIALS AND METHODS: Up-front bevacizumab-treated patients ($N = 38$) with newly diagnosed glioblastoma were analyzed by using an ADC histogram approach based on enhancing tumor. Using microarrays, we compared gene expression in high-versus-low ADC tumors in patients subsequently treated with bevacizumab. Tissue sections from a subset of tumors were stained for collagen and collagen-binding proteins. Progression-free and overall survival was determined by using Cox proportional hazard ratios and the Kaplan-Meier method with the log rank test.

RESULTS: A total of 13 genes were expressed at 2-fold or greater levels in high- compared with low-ADC tumors at the $P < .05$ level. Of these, 6 encode for collagen or collagen-binding proteins. High gene expression for the collagen-binding protein decorin was associated with shorter survival (HR, 2.5; $P = .03$). The pattern and degree of collagen staining were highly variable in both high- and low-ADC tumors.

CONCLUSIONS: High-ADC GBMs show greater levels of *ECM* protein gene expression compared with low-ADC GBMs. It is unclear whether this translates to the accumulation of higher levels of the encoded proteins. However, because ECM molecules could contribute to a proinvasive phenotype, this relationship merits further investigation.

ABBREVIATIONS: ADC_L = mean ADC (10^{-6} mm^2/s) of the lower curve from the histogram analysis; ECM = extracellular matrix; GBM = glioblastoma; HR = hazard ratio; NIH = National Institutes of Health; RNA = ribonucleic acid; RPA = recursive partitioning analysis; VEGF = vascular endothelial growth factor; VEGF-A = vascular endothelial growth factor-A

G BMs are the most aggressive and lethal primary brain tumors.[1] Diffusion-based imaging paradigms have the ability to interrogate tumor physiology and, though previously used for assessment of stroke, are currently being developed as biomarkers for tumors. For instance, ADC histogram analysis has been used to predict response to bevacizumab in patients with recurrent GBM,[2] and minimum ADC values have been found to be prognostic of outcomes in gliomas.[3,4]

Bevacizumab is a monoclonal antibody against VEGF-A, a primary mediator of angiogenesis in malignant gliomas.[5] In patients with recurrent GBM, bevacizumab regimen treatment has been shown to improve response rate, as well as progression-free and overall survival compared with historical controls.[6,7] It is known that the response to bevacizumab is highly variable, but the mechanisms underlying bevacizumab susceptibly are not well-characterized.[8,9] More recently, the effect of bevacizumab therapy has been studied when started within 3–6 weeks after maximal tumor resection, concurrent with radiation and temozolomide therapy (ie, "up-front" treatment). In this setting, although progression-free survival improved, no benefit to overall survival was found.[10,11]

Microarrays are a powerful tool used to characterize genome-wide gene expression based on messenger RNA levels in tumor and other tissue. This technique has been used to demonstrate correlations between gene-expression levels, MR imaging–derived imaging features, and outcomes in GBM.[12-14] This combination of imaging and gene expression, sometimes referred to as "radiogenomics," has the potential to give insight into tumor biology that would be difficult to acquire from either technique alone.[15]

In the current work, we investigated the relationship between an MR imaging–derived physiologic imaging parameter, in this case tumor ADC, and gene expression. Previously, it has been shown that ADC histogram analysis can stratify progression in patients with GBM treated up-front with bevacizumab.[16] Thus, we determined the gene expression differences between high- and low-ADC tumors in treatment-naïve GBM subsequently treated with bevacizumab, and the relationship of the differences to progression-free and overall survival.

Materials and Methods

Patients

All patients enrolled in this retrospective study signed institutional review board–approved informed consent agreeing to participate in

a study correlating image analysis with clinical outcomes. Data acquisition was performed in compliance with all applicable Health Insurance Portability and Accountability Act regulations. Patients were part of the AVF3770 study.[10,11] The study enrollment spanned May 2005 to November 2008. Patients ($N = 38$) received (6000 ± 200 cGy) external beam regional radiation started within 3–6 weeks after maximal tumor resection, concurrent with temozolomide and bevacizumab therapy. All patients met the following criteria: 1) pathology-confirmed GBM, 2) a baseline (presurgical) MR imaging scan that included diffusion-weighted images, 3) minimum 1 year of clinical follow-up, 4) age older than 18 years, 5) Karnofsky Performance Status ≥ 60, and 6) available microarray genomic data that were acquired from gross total or near-total ($>80\%$) resection in all except 1 patient based on the enhancing lesion. Follow-up scans were obtained at approximately 4- to 6-week intervals. Steroid doses for patients at the time of the initial scanning were not available in most cases. At the time of the last assessment (November 2010), 32/38 (84%) patients had died.

Imaging
MR imaging was performed on a 1.5T scanner and typically included axial T1-weighted (TR, 400 ms; TE, 15 ms; section thickness, 5 mm), T2-weighted fast spin-echo (TR, 4000 ms; TE, 126–130 ms; section thickness, 5 mm), FLAIR (TR, 8802 ms; TE, 122 ms; TI, 2100 ms; section thickness, 3 mm), diffusion-weighted and gadopentetate dimeglumine–enhanced (Magnevist; Berlex, Wayne, New Jersey; 0.1 mmol/kg) axial and coronal T1-weighted images (TR, 400 ms; TE, 15 ms; section thickness, 3 mm), with an FOV of 24 cm and a matrix size of 256×256. Postcontrast images were acquired immediately following contrast injection. Diffusion images used a section thickness of 3–5 mm, FOV of 24 cm, and matrix size of 256×256 for most patients. Most patients (32 of 38) were scanned either on a 1.5T Signa MR imaging unit (GE Healthcare, Milwaukee, Wisconsin) or on a 1.5T Sonata scanner (Siemens, Erlangen, Germany), by using the standard diffusion-weighted imaging pulse sequence supplied by the scanner manufacturer. This pulse sequence includes 1 image acquisition at $b = 0$ s/mm^2 and 3 diffusion-weighted acquisitions using $b = 1000$ s/mm^2.

Volume Acquisition/ADC Histograms
Enhancing tumor volumes were segmented on postcontrast T1-weighted images on presurgical scans by using a semiautomated adaptive thresholding technique so that all pixels above the threshold value were selected as previously described.[2] Therefore, significant regions of macroscopic necrosis that were not enhancing as well as cystic areas were excluded. The resulting ROIs encompassing the entire enhancing tumor volumes were verified by a board-certified neuroradiologist (W.B.P., 7 years of experience) blinded to clinical outcome and were mapped to the ADC images. ADC values calculated on a pixel-by-pixel basis for the entire enhancing volume were used for histogram analysis and expressed in units of 10^{-6} mm^2/s. ADC histograms were processed by using a 2-mixture normal distribution to provide optimal curve fitting as previously described.[2] Mean values for the lower peak (ADC$_L$, lower curve mean) were then generated, and tumors were dichotomized by using a cutoff for mean ADC$_L$ of 1200 based on prior work.[2] Tumors with mean ADC$_L$ < 1200 10^{-6} mm^2/s are referred to as "low-ADC tumors," whereas tumors with mean ADC$_L$ > = 1200 10^{-6} mm^2/s are referred to as "high-ADC tumors."

Determination of Tumor Progression
Progression-free survival from the time of tumor resection was determined on the basis of modified Macdonald criteria, in which nonenhancing tumor growth also was considered as evidence of tumor progression as per the Response Assessment in Neuro-Oncology working group.[17,18] Specifically, to increase sensitivity for nonenhancing tumor progression, 2 reviewers (W.B.P. and A.L.) retrospectively assessed the MR imaging and backdated time of progression to the earliest convincing worsening of FLAIR signal-intensity change compatible with nonenhancing tumor (this was done after the ADC histograms were generated to prevent unblinding of the reviewers). Discrepancies were resolved by consensus of the 2 readers. The main purpose of this retrospective method was to avoid increased progression-free survival due to failure to recognize progression (particularly nonenhancing progression) in the context of VEGF inhibition. Similarly, to decrease the chance that "pseudoprogression" would be characterized as true tumor growth, the first postoperative scan was used as the baseline and new areas of progressive contrast enhancement within the radiation field that developed within 3 months of the end of radiation therapy and then spontaneously resolved without change in treatment were assessed as "pseudoprogression."

Microarray Data
Gene-expression data used in this work had been previously generated for a molecular study of GBM.[19] Briefly, RNA was purified from fresh frozen tumor samples and was hybridized to U133 Plus 2.0 Arrays (Affymetrix, Santa Clara, California) for analysis of roughly 13,283 genes. The data files generated were normalized by using RMA from Bioconductor (for R, Version 2.6; http://cran.r-project.org/bin/windows/base/), relative to other Affymetrix microarrays of the same platform by using the Celsius data base (http://www.ncbi.nlm.nih-.gov/pubmed/17570842). RMA normalized data were imported into dChip (http://biosun1.harvard.edu/complab/dchip)[20] for differential expression analysis among genes in different ADC groups. We compared the fold change for the mean of each gene in the different ADC groups and used a t test to assess the significance. Significant genes were further analyzed by the DAVID bioinformatics tool (The US NIH data base for annotation, visualization, and integrated discovery; http://david.abcc.ncifcrf.gov)[21] to identify enriched biologic groups.

Immunohistochemistry
Immunohistochemistry was performed by using antibodies against collagen I, III, VI, and decorin in a series of 38 formalin-fixed paraffin-embedded GBM tumor samples, 1 set of samples from each patient. Immunostaining was measured quantitatively, evaluating the attenuation of collagen on a scale of 0–4: 0, none, no immunopositivity for collagen; 1, mild/scarce, immunopositive for collagen in <25% of the tumor area, including vascular, cytoplasmic and interstitial staining; 2, scarce to moderate, immunopositive for collagen in 25%–50% of the tumor area, including vascular, cytoplasmic, and interstitial staining; 3, moderate to extensive: immunopositive for collagen in 50%–75% of the tumor area, including vascular, cytoplasmic, and interstitial staining; 4, extensive, immunopositive for collagen in >75% of the tumor area, including vascular, cytoplasmic, and interstitial staining.

Immunohistochemistry was performed by using whole-slide quantification with Image Analysis software (Aperio Technologies, Vista, California) by using the Positive Pixel Count and Nuclear Al-

	Male ($n = 24$)	Female ($n = 14$)	All ($N = 38$)
Age (mean ± SD) (yr)	59.5 ± 9.2	54.9 ± 7.1	57.8 ± 8.7
Age range (yr)	42–75	42–67	42–75
Baseline mean ADC_L	1151 ± 169	1121 ± 162	1140 ± 165
Radiation dose (cGy)	5904 ± 378	5014 ± 2178	5576 ± 1394
Surgery type	G 13/24, S 11/24	G 5/14, S 9/14	G 18/38, S 20/38

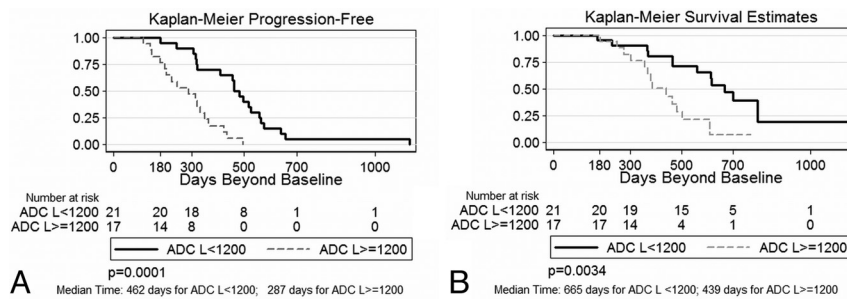**Note:**—G indicates gross total resection; S, subtotal resection or biopsy.

Fig 1. Kaplan-Meier progression-free (*A*) and overall (*B*) survival estimates for newly diagnosed patients with GBM treated up-front with bevacizumab on the basis of ADC histogram analysis of enhancing tumor from preoperative scans. High-ADC tumors are associated with poorer outcomes compared with low-ADC tumors.

gorithms. Positivity was calculated on the basis of the ratio of the Positive Pixel Count to the total number of pixels. Results were reviewed and confirmed by a neuropathologist (W.Y.) and neuropathology researcher (L.M.).

Statistical Methods

A test of the proportional hazards assumption was used after fitting uni- and multivariate Cox models, and 95% confidence intervals were generated. The Kaplan-Meier method with a log rank test was used to estimate progression-free survival. For all analyses, a *P* value of $< .05$ was accepted as significant. Statistical analysis was performed with Stata 10 2008 (StataCorp, College Station, Texas). The Fisher exact test was used to test gene expression data in which multiple probes showed >2-fold change at the 95% confidence level.

Results

Patient Characteristics and Survival

The patient cohort for this analysis ($N = 38$) represents a subset of patients used in previous studies ($N = 59$),[11,19] based on the availability of gene-expression data. For this subset, please see Table 1 for baseline patient characteristics and Fig 1 for survival analysis based on ADC histogram data. Note that high-ADC tumors have significantly shorter progression-free and overall survival compared with low-ADC tumors.

High-Versus-Low ADC Tumor Gene Expression

Gene-expression levels were compared between high- and low-ADC tumors to identify expression that may be related to the poorer prognosis seen with high-ADC tumors. Thus gene expression enriched in high-ADC tumors at the 2-fold or greater level compared with low-ADC tumors is shown in Table 2. Note that 6 of the 13 genes (some genes have multiple oligonucleotide probes used for the microarray analysis) increased in ADC tumors are either isoforms of collagen or collagen-binding proteins (collagen isoforms: *1A1, 3A1, 6A3,* and *11A1* and collagen-binding proteins: *decorin* and *lumican*). Multiple probes for *collagen 1A, 3A, 11A* and *decorin* were

elevated in the high-ADC tumors. With the Fisher exact test based on multiple probes, overexpression of *decorin* in the high- versus low-ADC tumors was significant at the $P = 9 \times 10^{-14}$ level. DAVID bioinformatics analysis confirmed the overexpression of *ECM*-related genes (not shown). When samples were ordered according to ADC_L values, there was a general trend of increasing extracellular matrix gene expression with increasing ADC. However, not all high-ADC tumors had high levels of *ECM* gene expression. This is illustrated in the heat map of gene expression levels (Fig 2). Only 3 genes were preferentially expressed in low-ADC compared with high-ADC tumors at the 2-fold or greater level. These are shown at the bottom of the heat map (Fig 2).

We also assessed gene expression individually to test whether this could stratify survival. We found that in a univariate analysis, increased *decorin* was associated with increased risk of death (Table 3), whereas *VEGF-A*, the target of bevacizumab, and *lumican* (another collagen-binding protein) did not predict outcome in the univariate model.

Histology: High-versus-Low ADC Tumors

Expression of decorin and collagen 1, 3 and 6 isoforms was highly heterogeneous by immunohistochemistry in both high- and low-ADC tumors (Fig 3). There was no significant correlation between ADC_L values and scoring of collagen immunoreactivity (*P* values ranging from .25 to .8). However, multiple patterns of immunoreactivity, including perivascular, interstitial, and cytoplasmic, were seen (Fig 3).

Discussion

ADC histogram analysis stratifies progression-free survival in patients with GBM subsequently treated with standard therapy and "up-front" bevacizumab, an inhibitor of tumor angiogenesis.[16] Treatment of gliomas with antiangiogenic therapy has been associated with a proinvasive phenotype that extends along blood vessels, so-called "vascular co-option."[22] It is also thought that this proinvasive phenotype may impart

Table 2: List of gene expression enriched >2-fold in high-versus-low ADC tumors at the *P* < .05 confidence level

Gene	Function	Low-ADC Mean	High-ADC Mean	Fold Change	P Value
COL11A1	Collagen[a]	100	257	2.56	.022
COL11A1	Collagen[a]	138	448	3.26	.028
COL1A1	Collagen[a]	714	2181	3.06	.017
COL1A1	Collagen[a]	84	347	4.13	.024
COL3A1	Collagen[a]	965	3152	3.27	.017
COL3A1	Collagen[a]	601	2020	3.36	.007
COL3A1	Collagen[a]	1229	3665	2.98	.014
COL6A3	Collagen[a]	296	648	2.19	.022
CXCL14	Chemokine	725	1607	2.22	.042
CYP1B1	Cytochrome	88	199	2.26	.018
CYP1B1	Cytochrome	246	582	2.36	.020
CYP1B1	Cytochrome	233	524	2.25	.032
DCN	Collagen-binding[a]	1014	2518	2.48	.013
DCN	Collagen-binding[a]	116	404	3.49	.019
DCN	Collagen-binding[a]	611	1583	2.59	.016
DCN	Collagen-binding[a]	582	1785	3.07	.022
KCNIP4	Potassium channel protein	125	259	2.08	.025
KIAA1576	Alcohol dehydrogenase	143	291	2.03	.015
LUM	Collagen-binding[a]	364	787	2.16	.032
MYLK	Myosin light chain kinase	522	1113	2.13	.006
RCAN2	Calcineurin pathway	154	442	2.86	.014
SLN	Sarcolipin	215	705	3.27	.025

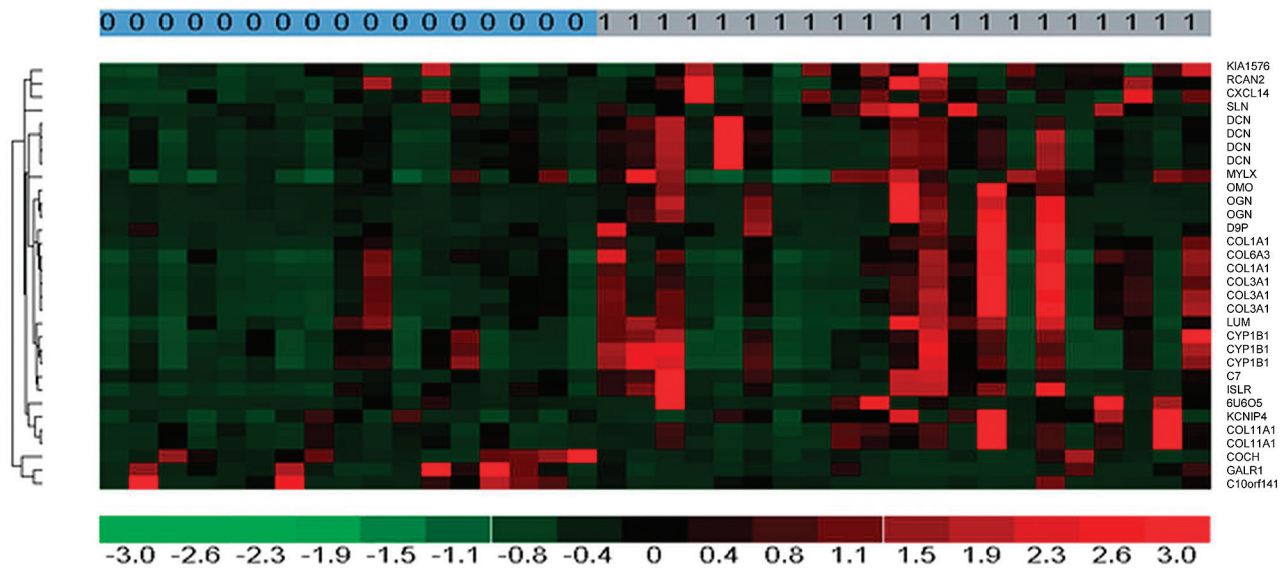[a] Note enrichment of collagen and collagen-binding gene expression.

Fig 2. Heat map (red corresponds to increased expression) showing gene expression in high-versus-low ADC tumors (1, top bar). Collagen isoforms and collagen-binding proteins are overexpressed in high-ADC tumors (right column, gene symbol). The bottom 3 genes were overexpressed in the low-ADC tumors.

Table 3: Univariate Cox model[a]

Model Covariate	HR	Z Score	P Value
VEGF-A (4 probes)	0.79	0.64	.52
DCN (5 probes)	2.5	2.23	.026[b]
LUM	0.89	−0.32	.75

[a] *Decorin* gene expression is associated with poor survival.
[b] Significant.

greater resistance to therapy and ultimately result in death. In the current report, we analyzed histopathologic and genomic differences between high- and low-ADC tumors in newly diagnosed GBM, to further characterize the relationship between ADC values and tumor biology in the setting of anti-angiogenic therapy.

The 38 patients in the present study represent a subset of those from our prior published work.[16] Progression-free and overall survival for this cohort was stratified by ADC histogram analysis as shown previously. Patients with high-ADC tumors had significantly poorer outcomes compared with those with low-ADC tumors. Therefore, we compared gene expression in the 2 groups, looking for genes whose expression was increased in the high-ADC (poorer survival) cohort. We found that 13 genes were overexpressed in high- compared with low-ADC tumors. Remarkably, 6 of these 13 genes encode for either collagen isoforms or collagen-binding proteins. Fibrillar collagens have previously been shown to be abundant but variably expressed in the extracellular matrix of GBM.[23] Collagen and other extracellular matrix proteins are
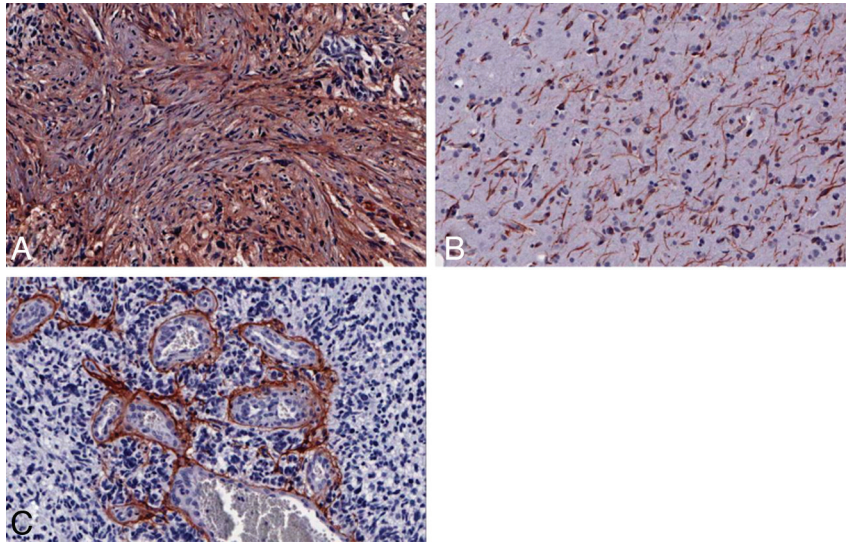
Fig 3. Patterns of immunohistochemical staining. *A*, Decorin, ×20. Note the interstitial pattern. *B*, Collagen 1, ×20. Note the cytoplasmic staining. *C*, Collagen 3, ×20. Note the perivascular staining.

thought to enhance tumor invasion. Epigenetic mechanisms have been described that allow gliomas to deposit an invasion-promoting collagen-enriched matrix and then to use this matrix to rapidly migrate through brain tissue. These collagen isoforms include *collagen 1A1*, 1 of the genes we found to be overexpressed in high-ADC (poor prognosis) tumors.[23,24]

As mentioned above, treatment with bevacizumab can result in tumor growth along established vasculature, potentially as a method of antiangiogenic treatment "escape." This perivascular pattern of invasion is also seen in an orthotopic mouse glioma model that overexpresses glutamate receptors. Overexpression of glutamate receptors results in increased glioma adhesion to collagen (reviewed in de Groot and Sontheimer, 2010[25]). Thus, several lines of evidence suggest a relationship between collagen deposition by gliomas and enhanced invasion. Therefore, it is interesting to speculate that high ADC tumors may occur more rapidly because they are more invasive, due to increased *ECM* deposition. However, when we assessed collagen expression by immunohistochemistry and trichrome staining in a subset of these patients, there did not appear to be a good correlation between collagen levels and ADC values. Therefore, the correlation between gene and protein expression levels and the relationship to ADC and survival require further evaluation.

We also found that gene expression for the collagen-binding proteins decorin and lumican were up-regulated in high-ADC tumors. Decorin is a small leucine-rich proteoglycan. Both decorin and lumican have been shown to act as tumor repressors by antagonizing tyrosine kinases receptors and inhibiting integrin receptors. This is thought to result in an antisurvival and proapoptotic response (reviewed by Theocharis et al[26]). Decorin has also been shown to be a potent trophic factor that protects neuronal progenitor cells and glioma cells from oxygen and glucose deprivation.[27] It has also been demonstrated that decorin expression is proportional to the quantity of tumor stroma; in patients with ovarian cancer, high decorin expression is associated with a higher incidence of relapse.[28] Furthermore, a dominant-negative mutation in U87 cells of the ischemic responsive enzyme "inositol-

requiring enzyme 1α" causes a 48-fold increase in *decorin* gene expression and is associated with a proinvasive and less angiogenic phenotype.[29] We found that increased levels of *decorin* gene expression levels were associated with shorter survival. Thus, there may be several mechanisms by which decorin could impact tumor progression. It might be that it is the balance of these factors that determine whether this is an overall net benefit or detriment to patient outcomes, and decorin expression may be tumor (or treatment) dependent.

We did not find a significant correlation between *ECM* gene expression and immunohistochemistry staining in selected paraffin sections. The reasons are unclear. While gene expression may be coupled to the rate of protein production, levels of protein staining would be affected by both the rate of protein production and degradation. Rates of ECM protein degradation may be increased in gliomas because proteinases such as matrix metalloproteinases that target collagen are known to be up-regulated in this disease.[30] Another potential explanation for this discrepancy is that in our study, tissue used for gene expression and that used for immunohistochemistry may have been from different areas of the tumor because stereotactic-derived biopsy tissue was not available. Additionally, microarray measures relative abundance of gene expression summed over the specimen, while immunohistochemistry reflects the percentage of tumor area with a signal intensity. This, in addition to the heterogeneity of GBM, may contribute to the decoupling of the 2 measures.

There are several caveats to our study, including those involved in ADC histogram generation as noted previously. These include variation in ADC values between different imaging platforms.[16] As is typically the case, steroid doses at the time of first imaging are always a challenge to acquire, and we were not able to do so for many patients. Steroid treatment reduces mean ADC by 7% in brain tumors,[31] and so the impact of steroids may not be great. Only small portions of tumors were available for histopathologic analysis, and GBMs are known to have significant regional variation. Thus the histology, as well as the samples used for gene expression, may not be representative of the tumor as a whole. Furthermore,

not all patients had enough tumor tissue for histopathologic analysis. Future, prospective work with stereotactic biopsies may help to diminish this potential source of error. Additionally, other diffusion parameters acquired from diffusion tensor imaging (which we did not perform) could be useful in understanding the relationship between collagen-related gene expression and tissue microstructure because these metrics are hypothesized to reflect adhesion molecules and cell structure in other necrotic lesions.[32]

Conclusions

We show the potential utility of combining imaging and genomics to understand tumor biology. High-ADC tumors overexpress genes for collagen and collagen-binding proteins, which could help promote a more invasive phenotype. Mechanisms of invasion are central to the poor prognosis of GBM and likely require a better understanding to improve patient outcomes.

References

1. Norden AD, Drappatz J, Wen PY. **Antiangiogenic therapies for high-grade glioma.** *Nat Rev Neurol* 2009;5:610–20
2. Pope WB, Kim HJ, Huo J, et al. **Recurrent glioblastoma multiforme: ADC histogram analysis predicts response to bevacizumab treatment.** *Radiology* 2009;252:182–89
3. Higano S, Yun X, Kumabe T, et al. **Malignant astrocytic tumors: clinical importance of apparent diffusion coefficient in prediction of grade and prognosis.** *Radiology* 2006;241:839–46
4. Oh J, Henry RG, Pirzkall A, et al. **Survival analysis in patients with glioblastoma multiforme: predictive value of choline-to-N-acetylaspartate index, apparent diffusion coefficient, and relative cerebral blood volume.** *J Magn Reson Imaging* 2004;19:546–54
5. Chamberlain MC. **Emerging clinical principles on the use of bevacizumab for the treatment of malignant gliomas.** *Cancer* 2010;116:3988–99
6. Friedman HS, Prados MD, Wen PY, et al. **Bevacizumab alone and in combination with irinotecan in recurrent glioblastoma.** *J Clin Oncol* 2009;27:4733–40
7. Kreisl TN, Kim L, Moore K, et al. **Phase II trial of single-agent bevacizumab followed by bevacizumab plus irinotecan at tumor progression in recurrent glioblastoma.** *J Clin Oncol* 2009;27:740–45
8. Pope WB, Lai A, Nghiemphu P, et al. **MRI in patients with high-grade gliomas treated with bevacizumab and chemotherapy.** *Neurology* 2006;66:1258–60
9. Wong ET, Brem S. **Antiangiogenesis treatment for glioblastoma multiforme: challenges and opportunities.** *J Natl Compr Canc Netw* 2008;6:515–22
10. Lai A, Filka E, McGibbon B, et al. **Phase II pilot study of bevacizumab in combination with temozolomide and regional radiation therapy for up-front treatment of patients with newly diagnosed glioblastoma multiforme: interim analysis of safety and tolerability.** *Int J Radiat Oncol Biol Phys* 2008;71:1372–80
11. Lai A, Tran A, Nghiemphu PL, et al. **Phase II study of bevacizumab plus temozolomide during and after radiation therapy for patients with newly diagnosed glioblastoma multiforme.** *J Clin Oncol* 2011;29:142–48
12. Kappadakunnel M, Eskin A, Dong J, et al. **Stem cell associated gene expression in glioblastoma multiforme: relationship to survival and the subventricular zone.** *J Neurooncol* 2010;96:359–67
13. Pope W, Chen J, Dong J, et al. **Relationship between gene expression and enhancement in glioblastoma multiforme: exploratory DNA microarray analysis.** *Radiology* 2008;249:268–77
14. Carlson M, Pope W, Horvath S, et al. **Relationship between survival and edema in malignant gliomas: role of vascular endothelial growth factor and neuronal pentraxin 2.** *Clin Cancer Res* 2007;13:2592–98
15. Rutman A, Kuo M. **Radiogenomics: creating a link between molecular diagnostics and diagnostic imaging.** *Eur J Radiol* 2009;70:232–41
16. Pope W, Lai A, Mehta R, et al. **Apparent diffusion coefficent histogram analysis stratifies progression-free survival in newly diagnosed bevacizumab-treated glioblastoma.** *AJNR Am J Neuroradiol* 2011;17:17
17. Wen PY, Macdonald DR, Reardon DA, et al. **Updated response assessment criteria for high-grade gliomas: response assessment in neuro-oncology working group.** *J Clin Oncol* 2010;28:1963–72
18. Macdonald DR, Cascino TL, Schold SC Jr, et al. **Response criteria for phase II studies of supratentorial malignant glioma.** *J Clin Oncol* 1990;8:1277–80
19. Lai A KS, Kharbanda S, Pope WB, et al. **Evidence for sequenced molecular evolution of IDH1 mutant glioblastoma from a distinct cell of origin.** *J Clin Oncol* 2011;29:4482–90
20. Pallini R, Ricci-Vitiani L, Banna G, et al. **Cancer stem cell analysis and clinical outcome in patients with glioblastoma multiforme.** *Clin Cancer Res* 2008;14:8205–12
21. Huang W, Sherman B, Lempicki R. **Systematic and integrative analysis of large gene lists using DAVID bioinformatics resources.** *Nat Protoc* 2009;4:44–57
22. de Groot JF, Fuller G, Kumar AJ, et al. **Tumor invasion after treatment of glioblastoma with bevacizumab: radiographic and pathologic correlation in humans and mice.** *Neuro Oncol* 2010;12:233–42
23. Huijbers I, Iravani M, Popov S, et al. **A role for fibrillar collagen deposition and the collagen internalization receptor endo180 in glioma invasion.** *PLoS One* 2010;5:e9808
24. Chernov AV, Baranovskaya S, Golubkov VS, et al. **Microarray-based transcriptional and epigenetic profiling of matrix metalloproteinases, collagens, and related genes in cancer.** *J Biol Chem* 2010;285:19647–59
25. de Groot J, Sontheimer H. **Glutamate and the biology of gliomas.** *Glia* 2010;29:29
26. Theocharis A, Skandalis S, Tzanakakis G, et al. **Proteoglycans in health and disease: novel roles for proteoglycans in malignancy and their pharmacological targeting.** *FEBS J* 2010;277:3904–23
27. Santra M, Katakowski M, Zhang R, et al. **Protection of adult mouse progenitor cells and human glioma cells by de novo decorin expression in an oxygen- and glucose-deprived cell culture model system.** *J Cereb Blood Flow Metab* 2006;26:1311–22
28. Newton T, Parsons P, Lincoln D, et al. **Expression profiling correlates with treatment response in women with advanced serous epithelial ovarian cancer.** *Int J Cancer* 2006;119:875–83
29. Auf G, Jabouille A, Guerit S, et al. **Inositol-requiring enzyme 1alpha is a key regulator of angiogenesis and invasion in malignant glioma.** *Proc Natl Acad Sci U S A* 2010;107:15553–58
30. Rao JS, Yamamoto M, Mohaman S, et al. **Expression and localization of 92 kDa type IV collagenase/gelatinase B (MMP-9) in human gliomas.** *Clin Exp Metastasis* 1996;14:12–18
31. Minamikawa S, Kono K, Nakayama K, et al. **Glucocorticoid treatment of brain tumor patients: changes of apparent diffusion coefficient values measured by MR diffusion imaging.** *Neuroradiology* 2004;46:805–11
32. Gupta RK, Nath K, Prasad A, et al. **In vivo demonstration of neuroinflammatory molecule expression in brain abscess with diffusion tensor imaging.** *AJNR Am J Neuroradiol* 2008;29:326–32